Satellite Products and Services Review Board

Algorithm Theoretical Basis Document: GCOM-W1/AMSR2 SDR Calibration

Compiled by the
GCOM-W1/AMSR2 EDR Team

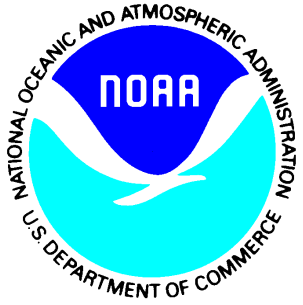

Version 1.0
February, 2014

AUTHORS:

Zorana Jelenak (UCAR)

Suleiman Alsweiss (GST)

Jun Park (CICS-MD/ESSIC)

Pat Meyers (CICS-MD/ESSIC)

Paul S. Chang (NOAA/NESDIS/STAR)

DOCUMENT HISTORY
DOCUMENT REVISION LOG

DOCUMENT TITLE: ATBD – GCOM-W1/AMSR2 SDR Calibration			
DOCUMENT CHANGE HISTORY			
Revision No.	**Date**	**Revision Originator Project Group**	**CCR Approval # and Date**
1.0	N/A	No version 1	N/A

LIST OF CHANGES

DOCUMENT TITLE: ATBD – GCOM-W1/AMSR2 SDR Calibration					
LIST OF CHANGE-AFFECTED PAGES/SECTIONS/APPENDICES					
Version Number	**Date**	**Changed By**	**Page**	**Section**	**Description of Change(s)**

TABLE OF CONTENTS

LIST OF ACRONYMNS

AMSR2: Advanced Microwave Sounding Radiometer 2
DDS: Data Distribution Server
EDR: Environmental Data Record
FOV: Field of View
GAASP: GCOM-W1 AMSR2 Algorithm Software Processor
GCOM – W1: Global Change Observation Mission 1st – Water
GPDS: GCOM Processing and Distribution System
JAXA: Japanese Aerospace Exploration Agency
SDR: Satellite Data Record
SST: Sea Surface Temperature
TMI: TRMM Microwave Imager
TRMM: Tropical Rainfall Measurement Mission

1. INTRODUCTION

Passive microwave radiometry is a special application of microwave communications technology for the purpose of collecting Earth's electromagnetic radiation. With the use of radiometers onboard earth orbiting satellites, engineers and scientists are able to monitor the Earth's environment and climate system on both short- and long-term temporal scales with near-global coverage [e.g. 1, 2]. Therefore, having well calibrated and stable microwave radiometers can provide unprecedented data to the scientific community for weather and climate research and operational activities.

The initial post-launch radiometer calibration and validation (Cal/Val) efforts commenced with the launch of the first Special Sensor Microwave Imager (SSM/I) on the Defense Meteorological Satellite Program (DMSP F-8) in 1987 [3] followed by a series of similar instruments (F-10 to F-15). The Naval Research Laboratory (NRL) led these Cal/Val activities aiming to study the stability of these instruments and their geolocation accuracy [4-6]. The identical design of the SSM/I instruments, provides a unique opportunity to directly compare near simultaneous observations from corresponding channels.

These inter-calibration efforts, which started 25 years ago, continue to be exploited to calibrate other spaceborne radiometers including the six SSM/I [7], two Special Sensor Microwave Imager/Sounder (SSMIS) [8], Tropical Rainfall Measuring Mission (TRMM) Microwave Imager (TMI) [9], the Advanced Microwave Scanning Radiometer for the Earth Observing System (AMSR-E) [10], and most recently the Global Precipitation Measurement (GPM) mission [11].

In May 2012, the Japanese Aerospace Exploration Agency (JAXA) successfully launched the Global Change Observation Mission-Water (GCOM-W1) with the Advanced Microwave Scanning Radiometer-2 (AMSR2) onboard. The observed brightness temperatures (Tbs) by AMSR2 will be used to infer several geophysical parameters and environmental data records (EDRs). Well calibrated AMSR2 Tbs will significantly improve the performance and accuracy of the geophysical retrieval algorithms and reduce retrievals errors. This document will demonstrate the basis of identifying and correcting residual calibration biases in AMSR2 Level 1B (L1B) Tbs with respect to TRMM Microwave Imager (TMI) as the reference radiometer.

2. INSTRUMENTS DESCRIPTION

Inter-calibration between sensors relies on finding collocated Tb measurements between different platforms. For sun-synchronous orbits, these collocation points generally occur only at higher latitudes near the poles [8], which greatly limits the amount of available data for inter-calibration. Thus, for a sun-synchronous radiometer like AMSR2 (local time of ascending node 13:30), a non-sun-synchronous, low inclination orbiter will create a larger amount of collocated observations to be used in the analysis. Therefore, TMI was chosen as the reference radiometer to study the calibration

biases of AMSR2. In the following subsections, some necessary background on the instruments design specifications for both AMSR2 and TMI are provided.

2.1. AMSR2

The GCOM program is part of JAXA's broader commitment toward global and long-term observation of the Earth's environment. The GCOM program consists of a series of two medium-size, polar-orbiting satellites with a planned one-year overlap between satellites in each series for inter-calibration. The two satellite series are GCOM-W (Water) and GCOM-C (Climate). Two instruments were selected as payloads for these missions to cover a wide range of geophysical parameters: AMSR2 on GCOM-W and the Second-generation Global Imager (SGLI) on GCOM-C. The AMSR2 instrument will perform observations related to the global water and energy cycle, while the SGLI will conduct surface and atmospheric measurements related to the carbon cycle and radiation budget [12].

The JAXA GCOM-W program was envisioned as a 13-year mission with three satellites in series, each with a 5-year lifetime including a 1-year overlap with the follow-on satellite for cross-calibration purposes. The GCOM-W1, launched in May 2012, will be followed by the GCOM-W2, and GCOM-W3 originally planned for launch in 2016, and 2020, respectively.

AMSR2 onboard GCOM-W1 is a microwave radiometer system that measures dual polarized [vertical (V-pol) and horizontal (H-pol)] radiances at 6.9, 7.3, 10.65, 18.7, 23.8, 36.5, and 89.0 GHz. It is a sun-synchronous orbiter that acquires microwave radiance data by conically scanning the Earth's surface to obtain measurements along a semicircular pattern in front of the spacecraft. It operates at a nominal earth incidence angle (EIA) of 55º that results in a wide swath of 1,450 km. The aperture diameter of AMSR2 antenna is 2.0 meters with an instantaneous field of view (IFOV) spatial resolution that varies inversely with frequency [13].

AMSR2 inherited most of AMSR-E characteristics with some important improvements including: a larger main reflector (compared to the 1.6m diameter of AMSR-E), the addition of the 7.3GHz channels (for C-band radio frequency interference (RFI) detection), 12 bit quantization for all channels, and improvements in the calibration system [14]. Summarized operating characteristics of AMSR2 are shown in Table 2-1 and the instrument design and geometry in Figure 2-1.

Table2-1. AMSR2 instrument specifications

Center Freq. (GHz)	Band Width (MHz)	Beam Width (3dB, deg.)	Ground IFOV (km)	Sampling Interval (km)
6.925/7.3	350	1.8	35×62	10
10.65	100	1.2	24×42	
18.7	200	0.65	14×22	
23.8	400	0.75	15×26	
36.5	1000	0.35	7×12	
89.0	3000	0.15	3×5	5

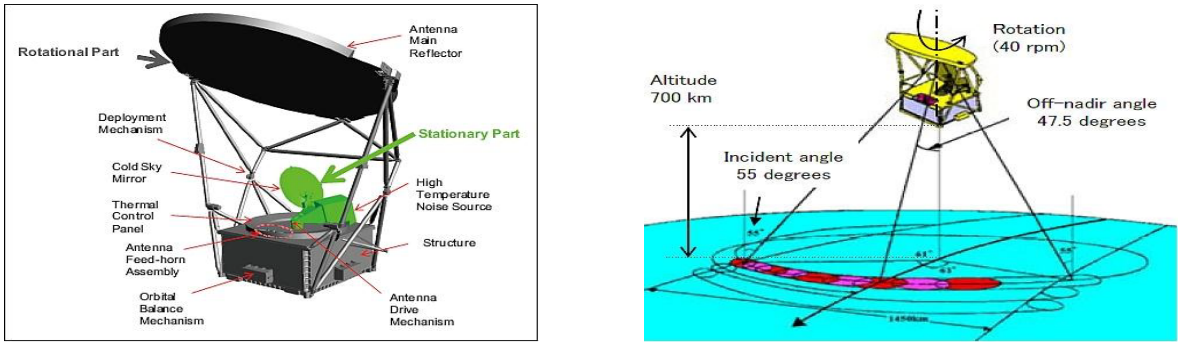

(a) (b)

Figure 2-1. Overview of AMSR2 (a) instrument design and (b) geometry (images credit: JAXA)

2.2. TMI

TMI is a conically scanning total power microwave radiometer, launched onboard TRMM in November 1997 into a near circular non-sun-synchronous orbit at a 350 km altitude with an inclination of 35º. In August 2001, TMI underwent an orbital boost, with new operating altitude of 402.5 km, to increase its operational lifetime. Now, it acquires data from an azimuth arc of 130º, at 53.2º nominal EIA, resulting in an 878 km swath. It has a total of nine radiometer channels: four dual polarized (V- and H-pol) measurements at frequencies of 10.65, 19.35, 37, and 85.5 GHz, and a single polarization measurement (V-pol only) at 21.3 GHz. The spatial resolution for individual measurements varies from 6 km at 85.5 GHz channels to 43 km at 10.65 GHz channels as shown in Table 2-2.

Table2-2. TMI instrument specifications

Center Freq. (GHz)	Band Width (MHz)	Polarization	Ground IFOV (km)
10.65	100	V/H	73×43
19.35	500	V/H	35×21
21.3	200	V	27×21
37.0	2000	V/H	19×10
85.5	3000	V/H	8×6

3. ALGORITHM DESCRIPTION

3.1 Theoretical Description

The inter-calibration methodology followed here to correct AMSR2 Tbs utilizes the double difference (DD) technique. The main advantage of the DD method is that it accounts for center frequency, EIA, and orbital differences between instruments being inter-calibrated. To calculate the DD, we need first to find the single difference (SD) for each radiometer, which is the difference between the observed and the simulated radiometer Tbs, with the latter generated using a radiative transfer model (RTM)) and supplementary data.

3.1.1 Observed Tbs

The AMSR2 data used are JAXA's Level 1B version 1.1 (GW1AM2 L1B v1.1) released on March 1, 2013. In addition to observed Tbs, this data product contains the observation position (latitude, longitude), time, and orbit information. The product summary and description is available online at [15]. The major modifications from the version 1.0 Tbs can be summarized as [16]: the correction of cold sky antenna temperature for 6.9 and 7.3 GHz V- and H-pol channels, the correction of hot load Tbs for all channels, and the updated antenna pattern correction (APC) coefficient for all channels.

For TMI, the data used herein are version 7 (v7) of the Level 1B Calibrated Tb product (TMI 1B11). The product summary and description for TMI 1B11 can be found in the Goddard Earth Sciences Data and Information Services Center (GES DISC) Web page [17]. The TMI 1B11 has gone through multiple revisions and improvements over TRMM's lifetime with the most recent, v7, in 2011. One of the changes from v6 to v7 was the implementation of time-varying solar bias correction [18, 19]. This TMI data product is available for public and can be downloaded using the Mirador Earth Science Data Search Tool [20] developed at the GES DISC.

3.1.2 Simulated Tbs

Modeling top-of-the-atmosphere brightness temperatures (Tb_{ToA}) using a microwave RTM is a key procedure in the calibration methodology implemented in this paper. For that purpose, we used the Joint Center for Satellite Data Assimilation (JCSDA) community RTM (CRTM) [21] version 2.1 with the Fast Microwave Ocean Emissivity Model (FASTEM) version 5.0 [22]. The CRTM consists of four main physical processes: the absorption of radiation by the gaseous constituents of the atmosphere, the absorption and scattering of radiation by clouds and aerosols, the surface emission of radiation and the surface interaction with downwelling atmospheric radiation. The result from the summation of these processes yields the simulated satellite sensor Tb_{ToA}.

To run the CRTM, we used the European Centre for Medium-Range Weather Forecasts (ECMWF) [23, 24]. These data are available every 6 hours (00Z, 06Z, 12Z, and 18Z) at 0.25º latitude/longitude (lat/lon) grid composed of 1440×720 grid boxes. The surface environmental parameters provided in the data are: hybrid level 1 surface pressure, sea surface temperature, surface skin temperature, and 10-m U and V wind components. The atmospheric environmental parameters are provided in 91 pressure levels and are as follows: height profiles of pressure, temperature, specific humidity, O3 mass mixing ratio, cloud ice water content, and cloud liquid water content.

ECMWF global fields were spatially and temporally interpolated to the sensor observation time and location. Afterwards, the interpolated surface and atmospheric parameters are fed to the CRTM along with the instrument frequency, polarization, and EIA to simulate Tb_{TOA}. Figure 3-1 shows a top-level block diagram for the simulation process used in this study.

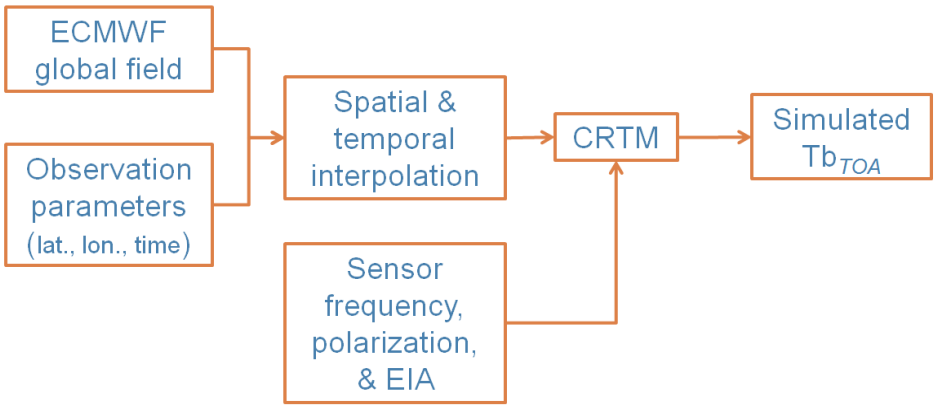

Figure 3-1. Top of atmosphere brightness temperature (Tb_{TOA}) simulation block diagram

3.1.3 Methodology

The simplest and most straight forward method for inter-calibration is the direct comparison of observed radiances from two radiometers. Unfortunately, even when the two radiometers being compared share the same center frequencies and nominal EIA, attitude control offset and different equatorial crossings will introduce different EIAs and diurnal variability. This might cause Tb differences that are not necessarily calibration errors.

The discrepancies of direct comparison can be mitigated by calculating the *SD* using simulated Tbs from an RTM as described in the previous section. The *SD*, defined in (3-1), minimizes the dynamic range of diurnal and seasonal cycle, and reduces the effect of EIA variability [25].

$$SD = Tb_{observed} - Tb_{simulated} \quad (3\text{-}1)$$

The most important characteristic of the RTM is that it captures the dynamic change of the ocean scene radiance due to changes in radiometer frequency, EIA, and polarization as well as changes in the environmental parameters. With the latter being derived from numerical weather models, they are imperfect estimates of the true values; hence RTM can not exactly represent the physics of the observation. However, through the use of *DD*, first order RTM errors, which are linear with the relevant parameters will tend to cancel. Second order errors will still show up in the *DD* analysis especially around the 23GHz water vapor absorption line. These second order errors can be mitigated by utilizing only clear-sky ocean scenes spanning long time periods for the calculation of the *DD*.

The *DD*, mathematically represented in (3-2), is calculated as the difference between the *SD*s of the two radiometers being inter-calibrated (AMSR2 and TMI in this study) on a channel-by-channel basis.

$$DD_{Freq.,Pol} = SD^{AMSR2}_{Freq.,Pol.} - SD^{TMI}_{Freq.,Pol.} \quad (3\text{-}2)$$

To perform AMSR2 inter-calibration with TMI, observations of the corresponding channels (frequency and polarization) from the two radiometers were collocated to establish a subset of ocean scenes (training dataset) that have homogeneous environmental conditions. For the training dataset, we used four months of collocated AMSR2 and TMI measurements (January-April, 2013), with a collocation criteria of 30 minutes maximum time difference, and 25 km maximum distance between the two sensors observations.

The training dataset is then filtered for rain and clouds to assure rain-free clear-sky observations. TMI environmental daily retrieval maps (version 4) provided by Remote Sensing Systems [26] were used for that purpose. Next, as an additional quality control (QC) procedure, more stringent constraints were applied on all channels. First, all points with a difference between observed and

simulated Tbs > 5 Kelvin were excluded to remove outliers. A probable cause for these outliers is either they are rain contaminated observed Tbs, or erroneous simulated Tbs possibly due to unrealistic modeled data. Second, if measured Tb values exceed the expected upper boundaries of brightness temperatures for rain-free ocean scenes, then these points were excluded from the training set. Third, AMSR2 ascending orbits are susceptible to significant sun glitter contamination. The additional QC procedure will eliminate these regions as much as possible using sun azimuth and elevation information provided in the GW1AM2 L1B data files. Figure 3-2 shows the difference between measured and simulated AMSR2 Tbs (K) for the 6 GHz V-pol channel, where sun glitter contaminated areas are encircled. Finally, an aggressive land mask is applied to remove any possible land contamination in the observed Tbs (100 km away from the coast).

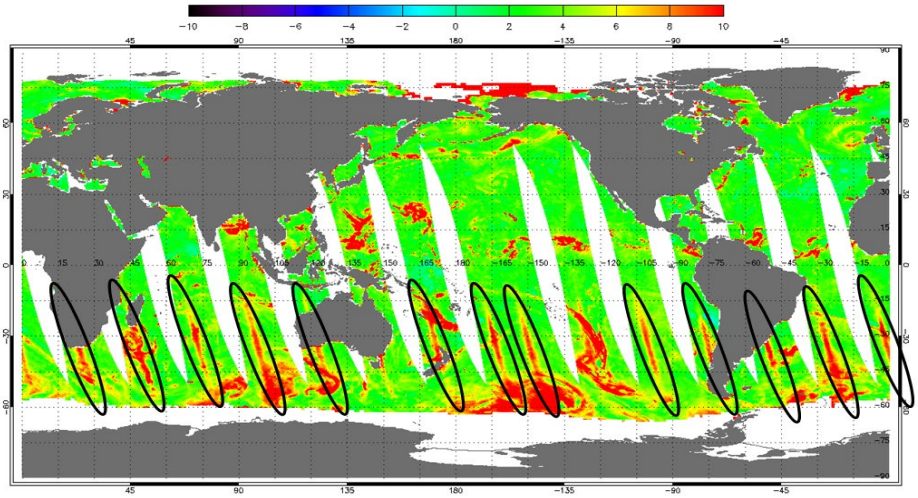

Figure 3-2. Sun glitter effect on AMSR2 ascending orbits.

Using the filtered training dataset (separated by frequency, polarization, and ascending/descending), the *DD* between AMSR2 and TMI was calculated as in (3-2). Table 3-1 shows the mean *DD* results for all AMSR2 channels with corresponding TMI counterparts. It clearly demonstrates that AMSR2 is measuring warmer Tbs than TMI.

Table3-1. AMSR2/TMI mean double difference

Channel	*DD* ascending, Kelvin	*DD* descending, Kelvin
10 GHz, V-pol	4.0	3.9
10 GHz, H-pol	4.6	4.7
18 GHz, V-pol	3.2	3.4
18 GHz, H-pol	1.8	1.9
23 GHz, V-pol	3.2	3.5
36 GHz, V-pol	3.5	3.6
36 GHz, H-pol	4.4	4.3
89a GHz, V-pol	1.1	1.1
89a GHz, H-pol	2.3	2.4
89b GHz, V-pol	0.7	0.8
89b GHz, H-pol	1.8	1.9

3.2 Mathematical Description

In order to correct AMSR2 calibration biases, the *DD* was mathematically modeled as a function of AMSR2 Tbs on a channel-by-channel basis. A second degree polynomial was used as shown in (3-3) to account for any possible non-linearity in the biases:

$$DD_{mod.} = ax^2 + bx + c \qquad (3\text{-}3)$$

where $DD_{mod.}$ is the modeled *DD,* and x is the observed Tb for each channel. Coefficients *a, b,* and *c* needed to reconstruct corrections are shown in table 3-2.

The modeled *DD* were then subtracted from AMSR2 measured Tbs ($Tb_{meas.}$) leading to corrected AMSR2 Tbs ($Tb_{cor.}$) as shown in (3-4).

$$Tb_{cor.} = Tb_{meas.} - DD_{mod.} \qquad (3\text{-}4)$$

Table 3-2. Modeled double difference equation coefficients

Channel	Ascending			Descending		
	a	***b***	***c***	***a***	***b***	***c***
10 GHz, V-pol	4.42×10^{-3}	-1.45	122.35	4.31×10^{-3}	-1.44	124.25
10 GHz, H-pol	2.02×10^{-3}	0.42	-16.35	4.78×10^{-3}	0.92	-39.67
18 GHz, V-pol	0.56×10^{-3}	-0.24	29.56	1.7×10^{-3}	-0.73	79.53
18 GHz, H-pol	6.47×10^{-5}	-0.07	9.79	0.55×10^{-3}	-0.20	18.10
23 GHz, V-pol	0.44×10^{-3}	-0.22	30.23	0.38×10^{-3}	-0.19	28.47
36 GHz, V-pol	1.33×10^{-3}	-0.57	64.27	1.66×10^{-3}	-0.71	80.48
36 GHz, H-pol	0.13×10^{-3}	-0.03	6.21	0.36×10^{-3}	-0.11	12.09
89a GHz, V-pol	2.77×10^{-3}	-1.41	181.26	3.43×10^{-3}	-1.76	227.10
89a GHz, H-pol	0.18×10^{-3}	-0.08	10.50	0.83×10^{-3}	-0.38	44.49
89b GHz, V-pol	3.27×10^{-3}	-1.66	212.41	3.51×10^{-3}	-1.79	229.40
89b GHz, H-pol	0.78×10^{-3}	-0.35	40.97	0.91×10^{-3}	-0.41	48.46

4. ALGORITHM IMPLEMENTATION

Algorithm was implemented operationally to correct AMSR2 L1B data in real time. The product is saved in files for every ascending and descending orbit in HDF5 format.

4.1 Input/output parameters

AMSR2 V1.1 Level 1B brightness temperatures are used as inputs for the algorithm, and it outputs SSW in m/s. The algorithm produces some quality flags indicating the retrievals accuracy.

4.2 Ancillary data

No ancillary data is needed after we determine the correction functions.

4.3 Assumptions

AMSR2 measurements are stable over time and different seasons.

4.4 Limitations

Currently, the predetermined correction functions were developed for land and ocean separately. A two-point absolute calibration approach with cold and hot ends might be a better way to characterize ASMR2 biases and will assure continuity over the whole Tb spectrum.

5. VALIDATION CONCEPT

In order to validate AMSR2 Tb corrections, they were applied on an independent (not used to derive biases) validation data set consisted of 1 month (June, 2013) of AMSR2/TMI collocations. Figures 5-1 and 5-2 demonstrate the DD maps for 10, 18, 23, 36, and 89 GHz V- and H-pol channels respectively, averaged over the validation data set time period. The left side panels show the DD maps before applying bias corrections to AMSR2 Tbs, where regions with warmer colors indicate the positive bias of AMSR2 Tbs. The right side panels show the DD maps after applying bias corrections (homogeneous with around zero mean). It is worth mentioning that collocations with TMI are limited in latitude and to ocean scenes only, hence the black regions.

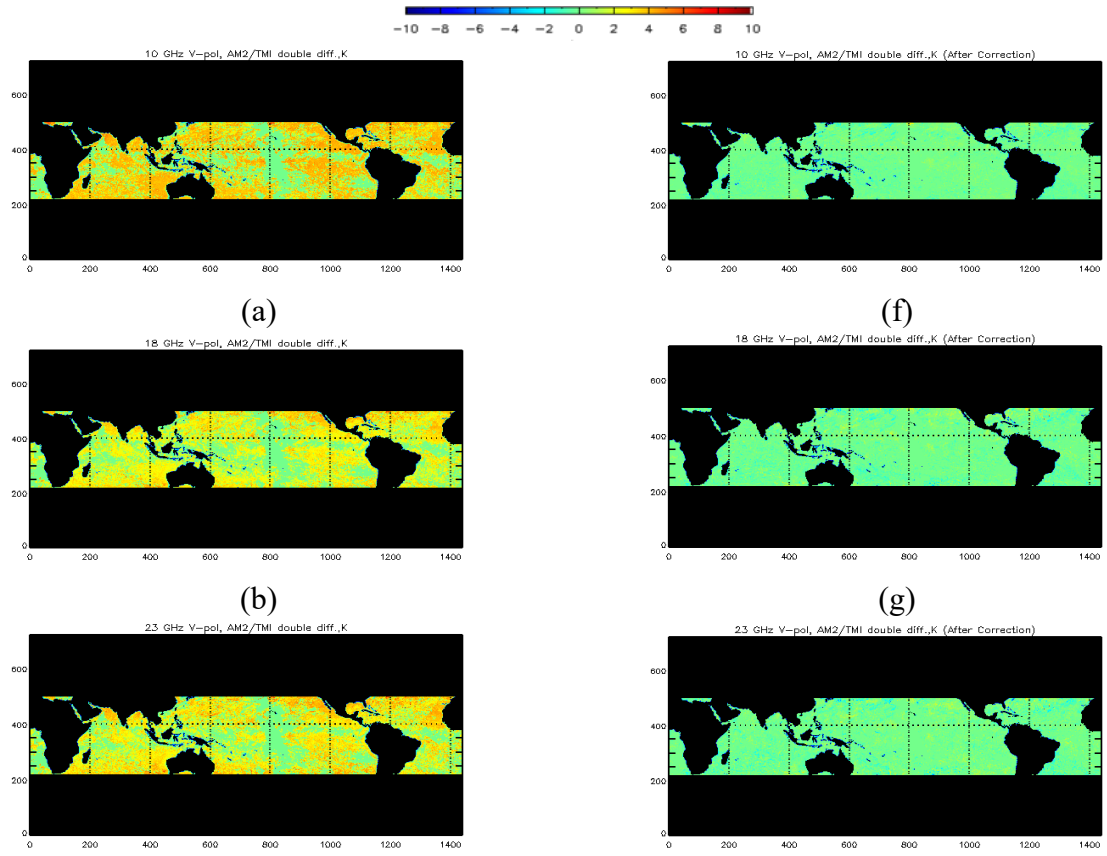

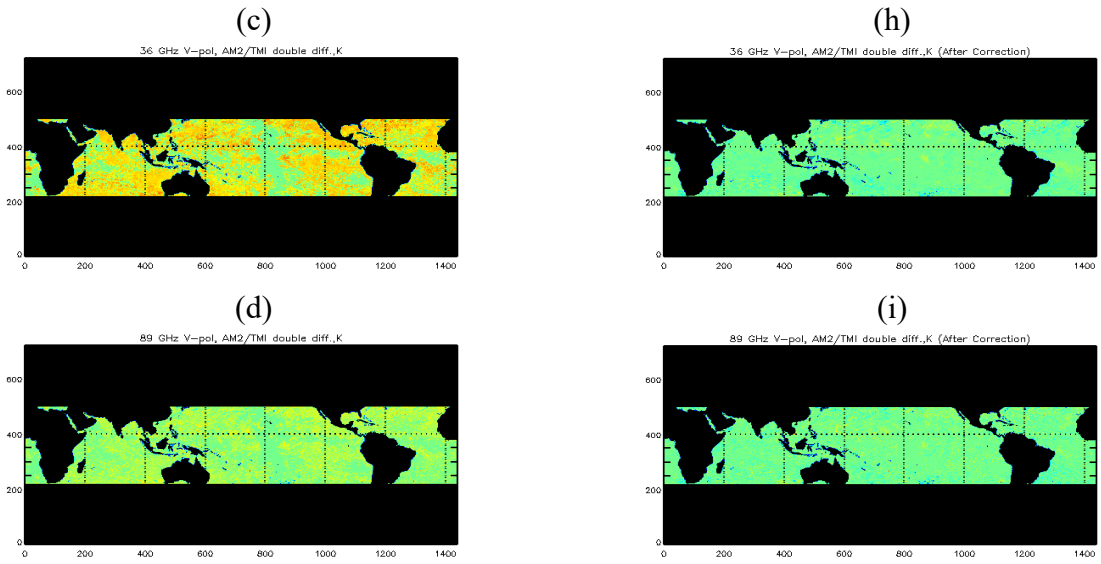

Figure 5-1. V-pol double difference maps for (a) 10 GHz, (b) 18 GHz, (c) 23 GHz, (d) 36 GHz, and (e) 89 GHz. Left side shows double difference maps before applying bias corrections to AMSR2 Tbs, and the right side shows the double difference maps after applying bias corrections.

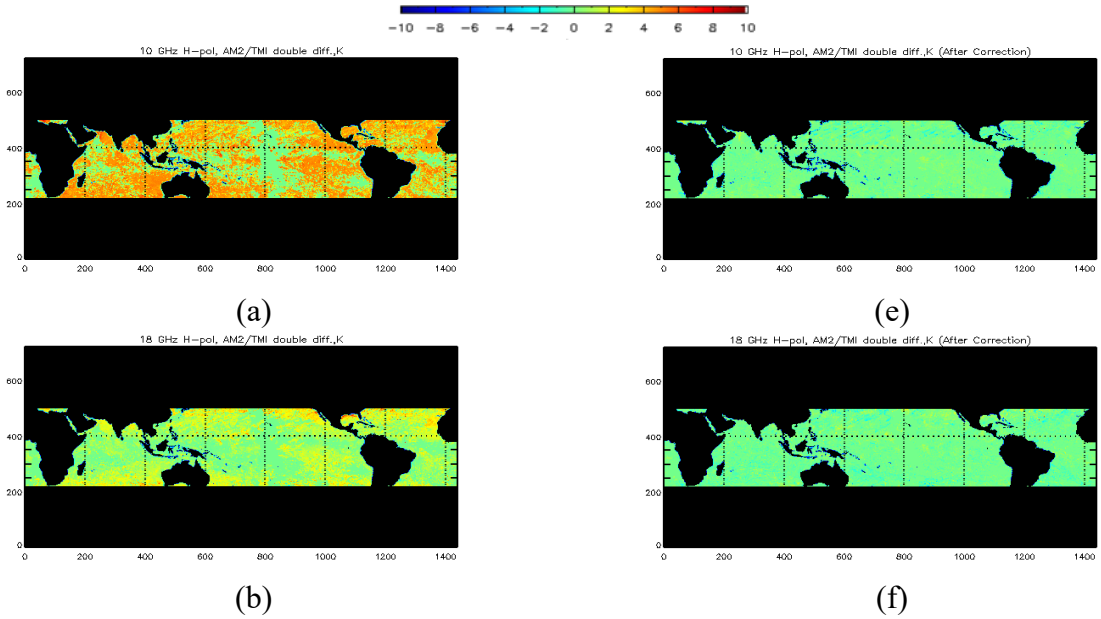

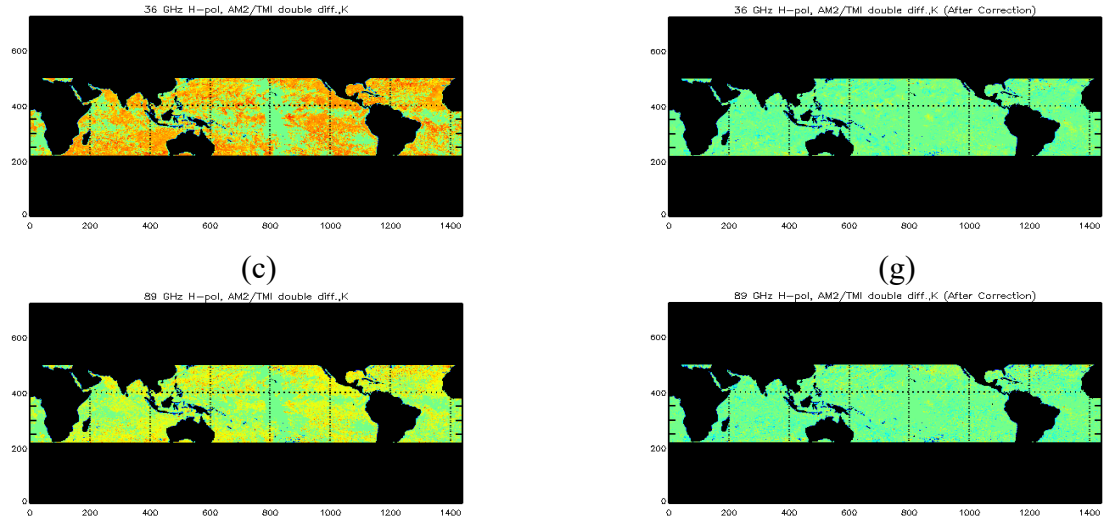

(c) (g)

(d) (h)

Figure 5-2. H-pol double difference maps for (a) 10 GHz, (b) 18 GHz, (c) 36 GHz, and (d) 89 GHz. Left side shows double difference maps before applying bias corrections to AMSR2 Tbs, and the right side shows the double difference maps after applying bias corrections.

Moreover, Fig. 5-3 compares the probability density functions (PDF) for AMSR2 DD results for both V- and H-pol channels. Left side panels (Fig. 5-3 a and b) show DD PDFs before applying bias corrections to AMSR2 Tbs, and the right side panels (Fig. 5-3 c and d) show the DD PDFs after applying bias corrections.

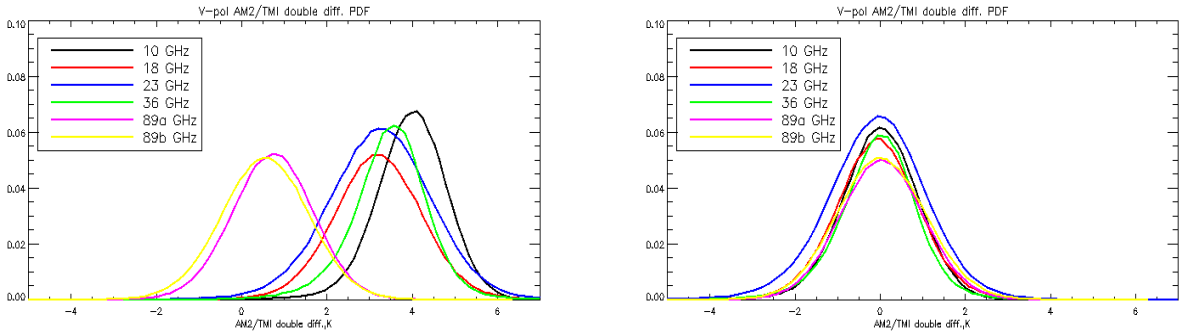

(a) (c)

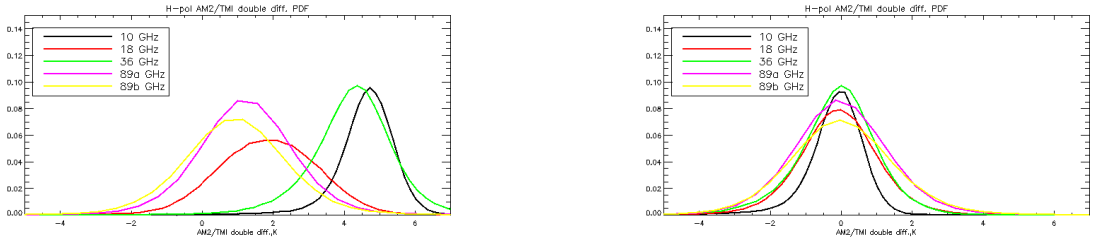

(b) (d)

Figure 5-3. AMSR2 double difference probability density functions for (a) V-pol, (b) H-pol, (c) V-pol after applying bias corrections, and (d) H-pol after applying bias corrections.

6. REFERENCES

[1] N. C. Grody, "Remote sensing of atmospheric water content from satellites using microwave radiometry," *IEEE Trans. Antennas Propagat.*, vol. AP-24, pp. 155–162, 1976.
[2] T. T. Wilheit and A. T. C. Chang, "An algorithm for retrieval of ocean surface and atmospheric parameters from the observations of the scanning multichannel microwave radiometer," *Radio Sci.*, vol. 15, pp.525–544, 1980.
[3] J. Hollinger, Ed., *DMSP Special Sensor Microwave Imager Calibration/Validation—Final Report*. Washington, DC: Naval Res.Lab., Jul. 1989.
[4] J. Hollinger, J. Peirce, and G. Poe, "SSM/I instrument evaluation," *IEEE Trans. Geosci. Remote Sens.*, vol. 28, no. 5, pp. 781–790, Sep. 1990.
[5] J. Hollinger, Ed., *DMSP Special Sensor Microwave Imager Calibration/Validation—Final Report*. Washington, DC: Naval Res. Lab., May 1991.
[6] M. Colton and G. Poe, "Intersensor calibration of DMSP SSM/I's: F-8 to F-14, 1987–1997," *IEEE Trans. Geosci. Remote Sens.*, vol. 37, no. 1, pp. 418–439, Jan. 1999.
[7] F. Wentz, "Inter-calibration of SSM/I F13, SSM/IS F16, and WindSat: A holistic approach (Invited)," *EOS Trans. AGU*, vol. 19, no. 26, 2010>, Ocean Sci. Meet. Suppl., Abstract IT24A-01.
[8] B. Yan and F. Weng, "Intercalibration between special sensor microwave imager/sounder and special sensor microwave imager," *IEEE Trans. Geosci. Remote Sens.*, vol. 46, no. 4, pp. 984–995, Apr. 2008.
[9] F. Wentz, P. Ashcroft, and C. Gentemann, "Post-launch calibration of the TRMM microwave imager," *IEEE Trans. Geosci. Remote Sens.*, vol. 39, no. 2, pp. 415–422, Feb. 2001.
[10] T. Meissner and F. Wentz, "Intercalibration of AMSR-E and Windsat brightness temperature measurements over land scenes," in *Proc. IEEE IGARSS*, Jul. 2010, pp. 3218–3219.
[11] S. Biswas, S. Farrar, K. Gopalan, A. Santos-Gracia, W. L. Jones, and S. Billanow, "Intercalibration of Microwave Radiometer Brightness Temperatures for the Global Precipitation Measurement Mission," *IEEE Trans. Geosci. Remote Sens.*, vol. 51, no. 3, pp. 1465–1477, Mar. 2013.
[12] Overview Of The Global Change Observation Mission (GCOM). [Online]. Available: http://suzaku.eorc.jaxa.jp/GCOM_W/w_amsr2/GCOM_RA_3rd_Guide_AppendixC.pdf
[13] JAXA GCOM-W1. [Online]. Available: http://suzaku.eorc.jaxa.jp/GCOM_W/w_amsr2/whats_amsr2.html
[14] K. Imaoka, M. Kachi, M. Kasahara, N. Ito, K. Nakagawa, and T. Oki, "Instrument Performance And Calibration Of Amsr-E And Amsr2," in *Proc. Int. Archives of the Photogrammetry, Remote Sensing and Spatial Information Science,* vol. XXXVIII, Part 8, Kyoto Japan 2010.
[15] AMSR2 Level1 Product. [Online]. Available: ftp://130.226.71.178/pub/Users/Leif.Toudal/PolarView/SGC-110038_AMSR2_Product_Format_Specification_Document(Level1)_draft.pdf
[16] GCOM AMSR2 V1.1 release. [Online]. Available: http://gcom-w1.jaxa.jp/130301_TBV1.1_release_e.pdf

[17] GES DISC Webpage for TMI 1B11 Data. [Online]. Available: http://mirador.gsfc.nasa.gov/collections/TRMM_1B11__007.shtml
[18] K. Gopalan, L. Jones, S. Biswas, S. Bilanow, T. Wilheit, and T. Kasparis, "A time-varying radiometric bias correction for the TRMM microwave imager," *IEEE Trans. Geosci. Remote Sens.*, vol. 47, no. 11, pp. 3722–3730, Nov. 2009.
[19] S. Biswas, K. Gopalan, W. Jones, and S. Bilanow, "Correction of time varying radiometric errors in TRMM microwave imager calibrated brightness temperature products," *IEEE Geosci. Remote Sens. Lett.*, vol. 7, no. 4,pp. 851–855, Oct. 2010.
[20] GES DISC Mirador Earth Science Data Search Tool. [Online]. Available: http://mirador.gsfc.nasa.gov/
[21] Y. Han, P. Van Delst, Q. Liu, F. Weng, B. Yan, R. Treadon, and J Derber, "JCSDA Community Radiative Transfer Model (CRTM) - Version 1," *NOAA Tech Report 122*, Washington, D.C, 2006.
[22] N. Bormann, A. Geer, and S. English, "Evaluation and comparisons of FASTEM versions 2 to 5," [Online]. Available: http://cimss.ssec.wisc.edu/itwg/itsc/itsc18/program/files/links/8.07_Bormann_pa.pdf
[23] A. Simmons, S. Uppala, D. Dee, and S. Kobayashi, "ERA-Interim: New ECMWF reanalysis products from 1989 onwards," ECMWF Newsletter 110: 26–35, 2006.
[24] J. Gibson, P. Kalberg, S. Uppala, A. Hernandes, A. Nomura, and E. Serrano, "ECMWF Reanalysis Report Series 1—ERA Description," ECMWF, 72 pp, 1997.
[25] R. A. Kroodsma, D. S. McKague, and C. S. Ruf, "Inter-calibration of Microwave Radiometers Using the Vicarious Cold Calibration Double Difference Method," *IEEE Journal of Selected Topics in Applied Earth Observations and Remote Sensing,*vol.5, no.3, pp.1006,1013, June 2012.
[26] Remote Sensing Systems. [Online]. Available: http://www.ssmi.com/tmi/tmi_description.html

END OF DOCUMENT